J. Mol. Model. **1999**, *5*, 90 – 96

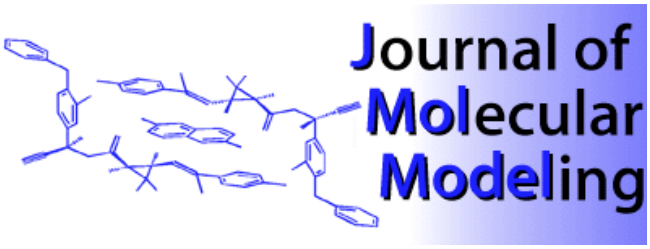

FULL PAPER

Molecular Modeling as a Powerful Tool for the Mapping of Fibroblast Growth Factor Receptor-1 Ligand Binding Determinants

Sérgio Oyama Jr., M. Terêsa M. Miranda, Sumika Kiyota, and Angelo G. Gambarini

Departamento de Bioquímica, Instituto de Química, Universidade de São Paulo, CP 26077, 05599-970, Sao Paulo, SP, Brasil. E-mail: aggambar@quim.iq.usp.br

Received: 8 December 1998/ Accepted: 11 February 1999/ Published: 14 April 1999

Abstract Molecular modeling has allowed us to propose that one main contact surface of the Fibroblast Growth Factor Receptor -1 (FGFR-1) to the ligand FGF-1 is formed by a 16 amino acid sequence comprised by the C-terminal region of the domain II (DII) plus the hinge linking DII and DIII domains and the N-terminal region of domain III (DIII). Therefore, this sequence was used to design the following three peptides: Ac-YQLDVVERS-NH_2 (R1); Ac-YQLDVVERSPHRPILQ-NH_2 (R2) and Ac-RSPHRPILQ-NH_2 (R3). The synthetic peptides were tested in their ability to inhibit the mitogenic activity of FGF-1 and FGF-2 in cultured Balb/c 3T3 fibroblasts. The results showed that R1 and R2 inhibited the activity of FGF-1 (ID_{50} = 40 –50 μM) but not that of FGF-2. Molecular modeling studies of R1 and its docking to FGF-1 suggested that this peptide could assume a conformation very similar to that found in the corresponding segment of FGFR-1. All these results support our hypothesis that the C-terminal residues of the DII domain, represented by peptide R1, are part of a surface responsible for the binding of FGF-1 to FGFR-1 but not of FGF-2. Also, they indicate that peptide R1 may be useful for the development of small selective peptide inhibitors of the FGF-1 biological activities.

Keywords Fibroblast Growth Factor, Receptor; Synthetic peptides, Mitogenic activity

Introduction

The Fibroblast Growth Factors (FGFs) are involved in the control of cell growth and differentiation, embryonic development, angiogenesis and malignant transformation.[1] These proteins act upon their target cells through the formation of a complex comprising the FGF molecule, the polysaccharide chain of heparan sulphate and the cell surface receptor.

Correspondence to: A.G. Gambarini

The FGF receptor (FGFR) belongs to a family of proteins composed by two or three extracellular immunoglobulin-like (Ig-like) domains, a single transmembrane chain and an intracellular domain with tyrosine kinase activity.[2] Upon FGF binding and receptor-dimerisation, the kinase domains of the FGFRs undergo cross-phosphorylations, resulting in signal transduction and biological response.[3]

Since there are no crystallographic coordinates for the extracellular domains of FGFRs, we have constructed a theoretical molecular model for the DII and DIII domains of FGFR-1, isoform β.[4] For that, we took into account data available in the literature showing that domains DII and DIII,

present in the β isoforms of FGFRs, are sufficient for FGF binding.[5, 6]

We have assembled a complex composed of: (I) one molecule of human FGF-1 (X-ray crystallographic coordinates) [7]; (II) one heparin dodecasaccharide (NMR coordinates of a synthetic fragment) [8] and (III) one set of the extracellular domains DII and DIII of FGFR-1β (theoretical model).[4] This structural analysis revealed a putative binding site for FGF-1 formed by a 16 amino acid sequence that comprises the C-terminal region of the DII Ig-like domain of FGFR-1 plus the hinge linking DII and DIII domains and the N-terminal region of DIII domain. The relevance of this sequence for FGF binding was evaluated by testing the ability of synthetic peptides R1, R2 and R3 to inhibit the mitogenesis promoted by FGF-1 and FGF-2.

Experimental procedures

Fibroblast Growth Factor

Recombinant human FGF-1 and bovine FGF-2 were produced and characterised as previously described by Gambarini and co-workers.[9] The samples used in the assays correspond to the 154 amino acids isoforms described for both factors.[10, 11]

Molecular modeling

Model building was performed on an IBM-RS6000 (3AT) workstation by using the BIOPOLYMER, HOMOLOGY, ANALYSIS and DOCKING modules of the INSIGHT II package.[12] Refinement of the model structures and other calculation steps were carried out *in vacuo* with the DISCOVER module of INSIGHT II, using the Consistent Valence Force Field (CVFF) [12] and a dielectric constant of 80.

Peptide synthesis, purification and characterisation

Peptides were synthesised manually employing p-methylbenzhydrylamine resin by the conventional solid-phase protocol described by Varanda and Miranda.[13] The t-Boc-L-amino acids were coupled using diisopropylcarbodiimide in dichloromethane (DCM) or in DCM/n-methylpyrrolidone (NMP) mixtures (1:1, v/v) for 1 h. When needed, the amino acid derivatives were recoupled or acetylation was carried out. The t-Boc deprotections were done using trifluoroacetic acid/DCM (TFA/DCM, 1:1, v/v) containing anisole. 10% triethylamine in DCM was used for the neutralisation steps. Couplings and recouplings were continuously monitored by the ninhydrin Kaiser test.[14] The peptide-resins were cleaved from the resin and fully deprotected with hydrogen fluoride (HF) containing 3% anisole at 0ºC for 1.5 h. The resulting crude peptides were purified by reversed-phase high performance liquid chromatography (RP-HPLC) using linear gradients of 0.1% TFA in 60% acetonitrile (ACN)/water and a C18 semi-preparative column. The purity of the peptides was evaluated by analytical RP-HPLC in TFA/ACN gradients. The purified peptides (> 90% pure) were characterised by amino acid analysis in a 6300 Beckman Analyser and by mass spectrometry.

Mitogenic assay

The stimulation of DNA synthesis was measured by the incorporation of [methyl-3H] -thymidine in Balb/c 3T3 fibroblasts, clone A31.[15] The cells were routinely grown in 10% FCS/DMEM (Fetal Calf Serum / Dulbecco's Modified Eagle Medium). For the assays, cells were incubated in 0.5% FCS/DMEM for 48 h. After this period, the medium was changed to serum-free medium containing 5μg/ml insulin. At the same time, growth factors and the synthetic peptides previously incubated (alone or in different combinations for 15 min at 37º C) were added to the culture medium. Twelve hours after stimulation [methyl-3H]-thymidine was supplied to the cells and the incorporation proceeded for the next 12 h. After this, the radioactivity incorporated in DNA

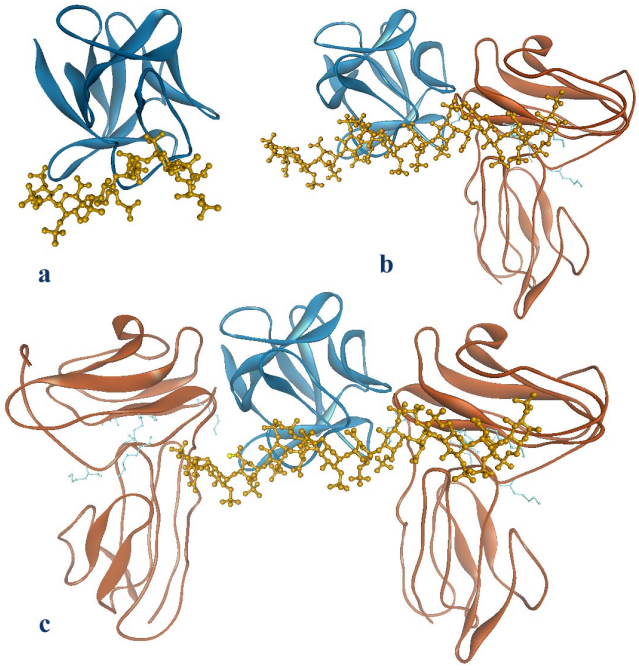

Figure 1 *Complex assembly. (a) human FGF-1 (blue)/Hexasaccharide (yellow). (b) Assembly of one human FGF-1 molecule, one Dodecasaccharide chain and one set of the DII/DIII extracellular domains of human FGFR-1-β (orange). (c) Final model consisting of 1 FGF-1-β Dodecasaccharide/2 FGFR-1*

was mearured. The assays were repeated at least five times. Responses are reported as percentages (% R) of that obtained in the presence of 10% FCS used as an internal control (100% R).

Results

Complex Assembly

Human FGF-1/Hexasaccharide FGF-1 and FGF-2 are the best characterised members of the FGF family. They are 55% identical in amino acid sequence and have very similar tertiary structures.[16] Previously reported data have shown that a hexasaccharide derived from heparin is active upon the FGF signalling system.[9, 17] Based on the available crystallographic coordinates for the complex human FGF-2/Hexasaccharide [18], we have constructed the analogous assembly human FGF-1/Hexasaccharide by superimposing the backbones of both FGFs as references. This first relative orientation of FGF-1/Hexasaccharide was decisive for the spatial positioning of the receptor binding sites in the FGF-1 molecule. The resulting complex (Figure 1a) was then used in the next step of the model building.

Human FGF-1/Dodecasaccharide/FGFR-1b The previously reported model for the extracellular domains of FGFR-1β [4] was then manually docked to the complex FGF-1/Hexasaccharide. This positioning was performed based on the hypothesis that the heparin binding sites of FGF-1 and FGFR-1 molecules form an almost continuous region able to bind about two repeats of the hexasaccharide molecule (Figure 1b). Hence, the hexasaccharide in the model was replaced by the NMR coordinates of one dodecasaccharide [8] by superimposing both fragments. Again, the resulting assembly was used in the next step described below.

Human FGF-1/Dodecasaccharide/2 FGFR-1b The relative spatial orientation of the FGF-1 in this complex allowed its interaction with a second FGFR-1 molecule according to the proposal of Pantoliano and co-workers [19] (Figure 1c). We can understand this assembly as the organisation of one FGF-1 and two FGFR-1 molecules along the axis formed by one glycosaminoglycan chain. The final model is supported by the experimental data summarised below.

The FGF heparin binding site has been characterised and in the FGF-1 molecule is composed by residues **N^{33}, N^{107}, K^{128}, Q^{132}, K^{133}** .[18, 20] Kan and co-workers [21] have proposed that there is also a heparin binding site in the FGFR molecule (residues **^{71}KMEKKLHAVPAAKTVKFK^{88}** in the FGFR-1β isoform). This segment corresponds to the two first β-strands of DII domain in the receptor model.[4] The spatial orientation of these residues results in the asymmetrical distribution of lysine side chains, which are involved with heparin binding, in both lateral surfaces of DII domain: there are two lysine side chains pointing to one side of the receptor and four oriented towards the opposite side (Figure 2). Potentially both lateral surfaces of the DII domain can bind the glycosaminoglycan chain, perhaps with different affinity. This creates an almost continuous heparin binding surface formed by the heparin binding site of FGF plus those of the two FGFRs (Figure 1c).

Mutagenesis studies [22] have identified a group of solvent-exposed residues that significantly contribute to the binding of FGF-2 to the receptor. The corresponding residues in the FGF-1 molecule are: **Y^{30}, R^{50}, N^{107}, Y^{109}, L^{148}, L^{150}** (Site 1, Figure 2). The authors have demonstrated that this is a high affinity binding site and heparin-independent. On the other hand, Site 2 [22, 23] (Figure 2) is a secondary binding site with about 250-fold lower affinity (corresponding residues in FGF-1: from **Y^{112}** to **F^{123}**) and is heparin-dependent. These characteristics are maintained in our model due to the spatial orientation of FGF-1, since the main contact Site 1/ loop 4 does not involve the dodecasaccharide. Conversely,

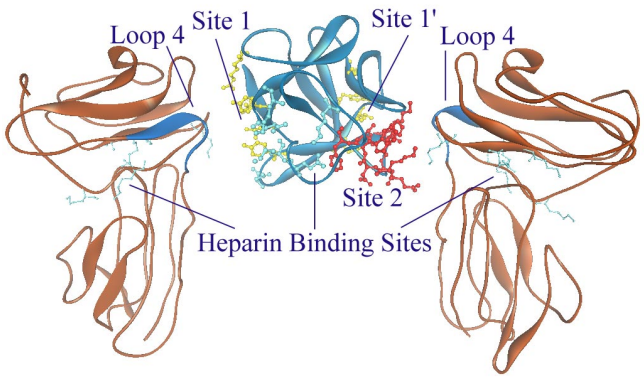

Figure 2 *Points of contact proposed for the formation of the FGF-1/FGFR-1 complex. The dodecasaccharide was removed and the receptor domains were drove apart for clarity*

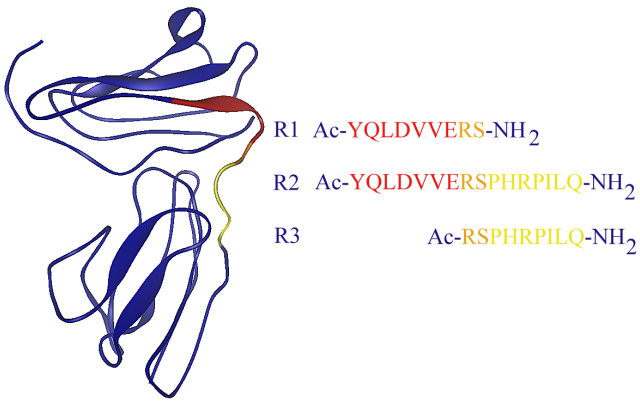

Figure 3 *Primary sequences and topological localization of the peptides R1 – R3 derived from FGFR-1*

the contact of Site 2 with the second FGFR-1 molecule is reinforced by the additional binding of heparin (Figure 1c).

The interacting surfaces in the complex revealed a new putative binding site located in the FGF-1 molecule. This region, which we call Site 1' (FGF-1: **Y^{70}, Y^{79}, L^{99}, L^{101}**; Figure 2), is similar to Site 1 in terms of amino acids composition. This is located in the opposite side of the molecule and therefore is an appropriate surface for the binding of a second FGFR-1 molecule in the complex, possibly through interaction with the loop 4 in the C-terminal region of DII domain of this second receptor molecule.

Interestingly, our model for the interactions in the complex FGF-1/FGFR-1/HS can be used to propose the formation of FGF-1/FGFR-1 oligomers of higher complexity (see Discussion and Figure 6).

Design of peptides related to the FGFR-1β sequence

We used the information described above to design peptides related to the FGFR-1β sequence that could bind to FGF-1 and inhibit its mitogenic activity. Peptides R1 - R3 (Figure 3) encompass a segment formed by the C-terminal region of the DII Ig-like domain of FGFR-1 (loop 4) plus the connective segment between DII and DIII domains and the N-terminal region of DIII domain. They were synthesised by the t-Boc solid-phase methodology [13], purified by RP-HPLC and characterised by analytical RP-HPLC, amino acid analysis and mass spectrometry.

Effect of peptides R1-R3 on the mitogenic activity of FGF-1 and FGF-2

The results obtained from the mitogenic assays of FGF-1 and FGF-2 in the presence of peptides R1 - R3 show that, in the range tested (1 to 600 μM), peptides R1 and R2 were able to inhibit the mitogenic activity of recombinant human FGF-1 (Figure 4a) without affecting that of recombinant bovine FGF-2 (Figure 4b). The inhibitory activity is dose-dependent in the range 10 to 100 μM for both peptides. This effect is sequence-dependent since peptide R3, corresponding to the C-terminal stretch of R2, was inactive. On the other hand, the N-terminal segment of peptide R2, represented by R1, is sufficient to elicit about the same response observed for the longer peptide R2 (ID_{50} = 40 –50 μM; Figure 4a). The inactivity of peptide R3 is in accordance with previous results showing that FGF-1 does not require this region for the binding to FGFR-1 mutants.[24]

Molecular modeling studies of peptide R1

Peptide R1 alone We performed a conformational search for peptide R1 through molecular dynamics simulations. In order to avoid fastidious and long time consuming runs we did not use the extended conformation of the peptide as a starting point. Alternatively, we adopted the conformation that is identical to that found in the corresponding segment of the FGFR-1 model structure, which is a β-hairpin.[4] We used the DISCOVER module of InsightII [12] to perform simulations at 300 K, during 100 ps (after a 15 ps equilibration step), using a dielectric constant ε = 80 and pH = 7.2.

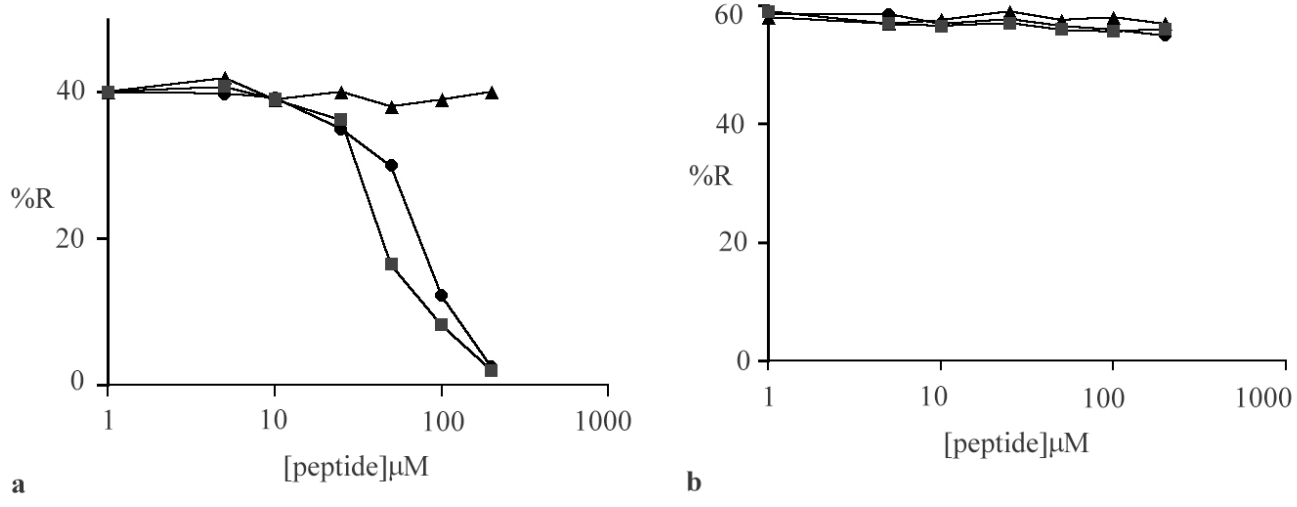

Figure 4 *Biological activity of the synthetic peptides. Different concentrations of peptides R1 (•), R2 (■) and R3 (▲) were pre-incubated with 50 pM of FGF-1 (a) or FGF-2 (b) for 15' at 37 °C and added to Balb/c 3T3 fibroblasts as described in the Experimental Section. Responses are represented as percentages (% R) of that obtained with 10% FCS (100% R)*

Data were collected every 1 ps and analysed with the ANALYSIS module.[12] The structures collected were grouped into families of similar conformations. This allowed us to verify that peptide R1 demonstrates a tendency to maintain the initial conformation along the simulation runs. The structure, which we called **"conformation A"**, is more rigid in the β-turn region (residues **D^{99}, V^{100} and V^{101}**) and more flexible in the extremities.

Docking of peptide R1 to FGF-1 The resulting structure for peptide R1 (**conformation A**) was then manually docked to the FGF-1 crystallographic coordinates [7] according to the orientation proposed in Figure 1b. The R1/FGF-1 complex was then submitted to molecular dynamics simulations at 300 K, pH = 7.2 and dielectric constant ε = 80. Analysis of the structures collected from 100 ps runs resulted in four representative families of conformations. In the next step, we used the DOCKING module of InsightII [12] to evaluate the interaction energies of peptide R1 relative to the FGF-1 molecule in the four families of conformations. This allowed us to perform a screening of the complexes and to choose which one resulted in the lowest interaction energy. This final complex (Figures 5a and 5b) showed an interaction energy 28.2 kcal/mol lower than that of the initial complex, manually docked. We denominated the final conformation of peptide R1 in the complex as **"conformation B"**.

Models comparison Both peptide R1 alone (**conformation A**) and peptide R1 (**conformation B**) docked to FGF-1 were further refined by a simulated annealing procedure. Calculations started at 300 K for 20 ps, then the structures were cooled in 50 K intervals down to 50 K, followed by a 25 K step and, finally, by a 10 K step. Every cooling step was preceded by equilibration for 0.5 ps with subsequent cooling over 5 ps. CVFF default cross terms were included in the two last steps. The temperature was regulated by velocity scaling. The energies of the resulting structures were minimised with the Steepest Descent algorithm followed by the Conjugated Gradient algorithm until energy variations up to 0.1 kcal/mol.Å and 0.05 kcal/mol.Å, respectively, were achieved.

When we compare the energies of **conformation B** for peptide R1 (separated from FGF-1) and **conformation A** (peptide alone), we observe an energy lowering of 37.3 kcal/mol, indicating that **conformation B** is more stable. In addition, this conformation is very similar to that found in the corresponding segment of FGFR-1. Also, there is a good adjustment of the accessible surface areas in the interface R1/Site 1 of FGF-1 (Figure 5a). The main interacting residues in this region are: **D^{99}, V^{100} and V^{101}** (R1) and **Y^{30}, R^{50}, Y^{109}, L^{148}, L^{150}** (FGF-1; Figure 5b). The side chains of residues **D^{99}** (R1) and **R^{50}** (FGF-1) are oriented properly for the formation of a salt bridge. Residues **V^{100} and V^{101}** (R1) and **Y^{30}, Y^{109}, L^{148}, L^{150}** (FGF-1) form an area of contact probably stabilised by hydrophobic interactions (Figures 5a and 5b).

Discussion

The main binding site (s) for FGF-1 are located in DII domain of FGFR (s)

Our results suggest that amino acid residues contained in peptide R1 are responsible, at least in part, for the binding of FGF-1 to FGFR-1 but not of FGF-2. Likewise, the major high affinity binding sites for FGF-1 (acidic FGF) and FGF-7 (Keratinocyte Growth Factor; KGF) reside within different

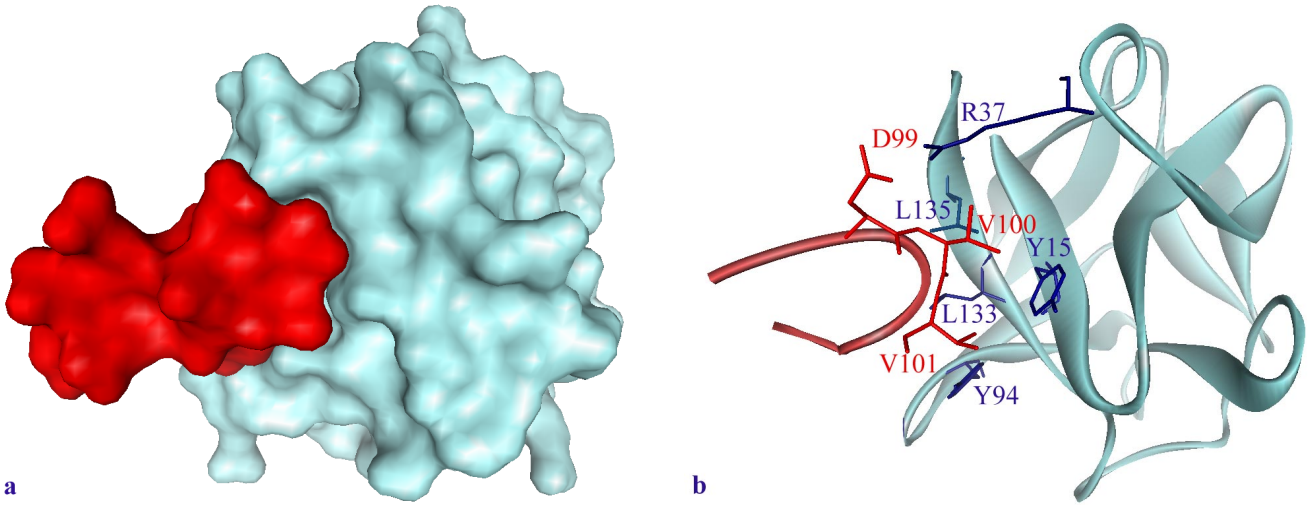

Figure 5 *Docking of peptide R1 to human FGF-1. (a) Spatial complementarity of the accessible surface areas for peptide R1 (red) and FGF-1 (blue). (b) Side chains interactions in the interface R1/Site 1 of FGF-1. The spatial orientation of the complex in both figures is the same*

Ig-like domains (DII and DIII, respectively) of FGFR-2-IIIb (KGFR).[25] In addition, a double mutation of FGFR-2-IIIb increased significantly the affinity for FGF-2 (basic FGF) without altering the affinity for FGF-7 and FGF-1. Conversely, a mutant of FGFR-2-IIIc in which the D-E loop is replaced by the FGFR-2-IIIb D-E loop displays a reduced affinity for FGF-2.[25] In fact, alternative splicing of exons IIIb and IIIc in the FGFR-2 gene alters specificity for FGF-2 and FGF-7 but not for FGF-1.[5, 27, 28]

FGF-1 non-specificity is related to its main binding site (s)

FGF-1 is a good ligand for IIIb/IIIc isoforms in the FGFRs family from 1 to 4.[29] Our model of complex formation (Figure 2) suggest that one of the most important binding site for FGF-1 is loop 4 in the DII domain, a well conserved region in all isoforms of FGFRs.[2] Therefore, FGF-1 is unspecific because, unlike FGF-2, it does not interact significantly with the more variable DIII domain, which is the most important determinant of specificity for the FGFs [29], or with the hinge connecting the DII and DIII domains [24] (Figure 4a).

FGF-1/FGFR-1 main interaction occurs between Site 1 and Loop 4

Recently, DiGabriele and co-workers [30] obtained three-dimensional coordinates for the complex of a decasaccharide of heparin with a trans-dimer of FGF-1. The authors did not propose an FGF binding site in the receptor molecule. Also, their schematic model for receptor dimerisation is different from ours (Figure 2). Nevertheless, our theoretical and experimental data indicate that, in both models, the binding of FGF-1 to FGFR-1 can be explained by an interaction between Site 1 of FGF-1 and loop 4 of the DII domain of FGFR-1. As far as we know, this is the first time that this specific receptor-ligand interaction has been proposed and experimentally tested.

Models for FGF-1/FGFR-1 oligomerisation

Alternative complexes for the formation of FGF-1/FGFR-1 oligomers can be built easily starting either from our model (Figure 2) or from the FGF dimer model proposed by DiGabriele and co-workers [30] by simple rotations and translations of FGFs or FGFRs along the axis formed by the sulphated glycosaminoglycan chain of one heparan sulphate or heparin molecule (Figure 6). Oligomerisation has been described for other receptors like Transforming Growth Factor-β (TGF-β) and Tumour Necrosis Factor-β (TNF-β) receptors [31, 32] and certainly would add more versatility for signalling modulation in the FGF complex.

Finally, peptide R1 seems to be an interesting peptide to develop specific inhibitors of FGF-1 activity.

Acknowledgements The authors wish to thank Dr. K. Kitagawa (Niigata College of Pharmacy, Niigata, Japan) for the mass spectrometry analyses and to C. W. Liria and I. N. Toma for technical assistance. This work was supported by grants from FAPESP, FINEP and CNPq.

Abbreviations FGF, fibroblast growth factor; FGFR, fibroblast growth factor receptor; Ig-like, immunoglobulin-like; DCM, dichloromethane; NMP, n-methylpyrrolidone; TFA, trifluoroacetic acid; HF, hydrogen fluoride; RP-HPLC, reversed-phase high performance liquid chromatography; ACN, acetonitrile; FCS, fetal calf serum; DMEM, Dulbecco's modified Eagle medium; HS, heparan sulfate; ID50, half-maximal inhibitory dose.

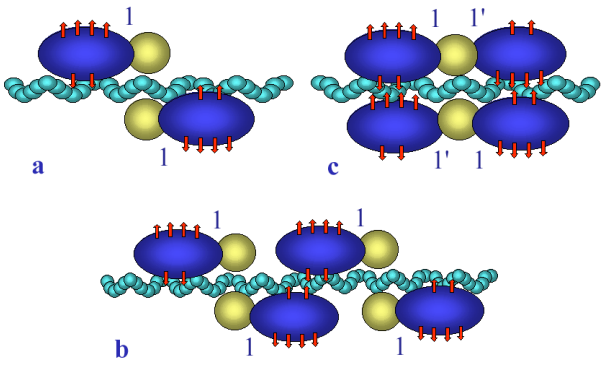

Figure 6 *Schematic representation of alternative FGF-1/FGFR-1 oligomers. These models were built based on: (a) a FGF-1 dimer [30]; (b) one FGF-1 high affinity binding site (Site 1); and (c) two FGF-1 high affinity binding sites (Figure 2). The schemes correspond to a top view of the complex orientation shown in Figure 2. The molecules are colored: FGF-1: yellow; FGFR-1: dark blue; glycosaminoglycan chain: light blue; lysine side chains: red. The proposed contact points Site1/loop4 and Site 1'/loop4 are indicated as 1 and 1' respectively*

References

1. Baird, A.; Klagsbrun, M. *Cancer Cells*, **1991**, *3*, 239.
2. Johnson, D. E.; Williams, L. T. *Advances in Cancer Research*, **1993**, *60*, 1.
3. Bellot, F.; Crumley, G.; Kaplow, J. M.; Schlessinger, J.; Jaye, M.; Dionne, C. A. *EMBO J.*, **1991**, *10*, 2849.
4. Oyama Jr., S.; Kiyota, S.; Miranda, M. T. M.; Gambarini, A. G; Viviani, W. *Journal of Molecular Modeling*, **1997**, *3*, 233.
5. Miki, T.; Fleming, T. P.; Bottaro, D. P.; Rubin, J. S.; Ron, D.; Aaronson, S. A. *Science*, **1991**, *251*, 72.
6. Wang, F.; Kan, M.; Xu, J.; Yan, G.; McKeehan, W. *J. Biol. Chem.*, **1995**, *270*, 10222.

7. Blaber, M.; DiSalvo, J.; Thomas, K. A. *Biochemistry*, **1996**, *35*, 2086.
8. Mulloy, B.; Forster, M. J.; Jones, C.; Drake, A. F.; Johnson, E. A.; Davies, D. B. *Biochem. J.*, **1993**, *293*, 849.
9. Gambarini, A. G.; Miyamoto, C. A.; Lima, G. A.; Nader, H. B.; Dietrich, C. P. *Mol. Cell. Biochem.*, **1993**, *124*, 121.
10. Jaye, M.; Howk, R.; Burgess, W.; Ricca, G. A.; Chiu, I. -M.; Ravera, M. W.; O'Brien, S. J.; Modi, W. E.; Maciag, T.; Drohan, W. N. *Science*, **1986**, *233*, 541.
11. Abraham, J. A.; Mergia, A.; Whang, J. L.; Tumolo, A.; Friedman, J.; Hjerrild, K. A.; Gospodarowicz, D.; Fiddes, J. C. *Science*, **1986**, *233*, 545.
12. Biosym/Molecular Simulation Inc., San Diego, CA
13. Varanda, L. M.; Miranda, M. T. M. *J. Pept. Res.*, **1997**, *50*, 102.
14. Kaiser, E.; Colescott, R. L.; Bossinger, C. D.; Cook, P. I. *Anal. Biochem.*, **1970**, *34*, 595.
15. Oyama Jr., S.; Miranda, M. T. M.; Toma, I. N.; Viviani, W.; Gambarini, A. G. *Biochem. Mol. Biol. Int.*, **1996**, *39*, 1237.
16. Zhu, X.; Komiya, H.; Chirino, A.; Fahan, S.; Fox, G. M.; Arakawa, T.; Hsu, B. T.; Rees, D. C. *Science*, **1991**, *251*, 90.
17. Barzu, T.; Lormeau, J. C.; Petitou, M.; Michelson, S.; Choay, J. *J. Cell. Physiol.*, **1989**, *140*, 538.
18. Faham, S.; Hileman, R. E.; Fromm, J. R.; Linhardt, R. J.; Rees, D. C. *Science*, **1996**, *271*, 1116.
19. Pantoliano, M. W.; Horlick, R. A.; Springer, B. A.; VanDyk, D. E.; Tobery, T.; Wetmore, D. R.; Lear, J. D.; Nahapetian, A. J.; Bradley, J. D.; Sisk, W. P. *Biochemistry*, **1994**, *33*, 10229.
20. Thompson, L. D.; Pantoliano, M. W.; Springer, B. A. *Biochemistry*, **1994**, *33*, 3831.
21. Kan, M.; Wang, F.; Xu, J.; Crabb, J. W.; Hou, J.; McKeehan, W. L. *Science*, **1993**, *259*, 1918.
22. Springer, B. A.; Pantoliano, M. W.; Barbera, F. A.; Gunyuzlu, P. L.; Thompson, L. D.; Herblin, W. F.; Rosenfeld, S. A.; Book, G. W. *J. Biol. Chem.*, **1994**, *269*, 26879.
23. Baird, A.; Schubert, D.; Ling, N.; Guillemin, R. *Proc. Natl. Acad. Sci. USA*, **1988**, *85*, 2324.
24. Wang, F.; Kan, M.; McKeehan, K.; Jang, J. H.; Feng, S.; McKeehan, W. L. *J. Biol. Chem.*, **1997**, *272*, 23887.
25. Cheon, H.-G.; LaRochelle, W. J.; Bottaro, D. P.; Burgess, W. H.; Aaronson, S. A. *Proc. Natl. Acad. Sci. USA*, **1994**, *91*, 989.
26. Gray, T. E.; Eisenstein, M.; Shimon, T.; Givol, D.; Yayon, A. *Biochemistry*, **1995**, *34*, 10325.
27. Werner, S.; Duan, D.-S. R.; de Vries, C.; Peters, K. G.; Johnson, D. E.; Williams, L. T. *Mol. Cell. Biol.*, **1992**, *12*, 82.
28. Yayon, A.; Zimmer, Y.; Guo-Hong, S.; Avivi, A.; Yarden, Y.; Givol, D. *EMBO J.*, **1992**, *11*, 1885.
29. Ornitz, D. M.; Xu, J.; Colvin, J. S.; McEwen, D. G.; MacArthur, C. A.; Coulier, F.; Gao, G.; Goldfarb, M. *J. Biol. Chem.*, **1996**, *271*, 15292.
30. DiGabriele, A. D.; Lax, I.; Chen, D. I.; Svahn, C. M.; Jaye, M.; Schlessinger, J.; Hendrickson, W. A. *Nature*, **1998**, *393*, 812.
31. Massagué, J. *Nature*, **1996**, *381*, 620.
32. Banner, D. W.; D'arcy, A.; Janes, W.; Gentz, R.; Schoenfeld, H-J.; Broger, C.; Loetscher, H.; Lesslauer, W. *Cell*, **1993**, *73*, 431.